# Terpenoids for medicine

Fischedick, J.

# Chapter 7

# Structure activity relationship of phenolic diterpenes from *Salvia officinalis* as activators of the antioxidant response element

Justin T Fischedick[a,b,*], Miranda Standiford[c], Delinda A. Johnson[c], Jeffrey A. Johnson[c]

[a]*PRISNA BV, Einsteinweg 55, 2300 RA Leiden, Netherlands*
[b]*Natural Products Laboratory, Institute of Biology, Leiden University, 2300 RA Leiden, The Netherlands*
[c]*Division of Pharmaceutical Sciences, School of Pharmacy, University of Wisconsin, Madison, WI, USA*

**Abstract**

Nuclear factor E2-related factor 2 is a transcription factor known to activate cytoprotective genes which may be useful in the treatment of neurodegenerative disease. In order to better understand the structure activity relationship of phenolic diterpenes from *Salvia officinalis* L., we isolated carnosic acid, carnosol, epirosmanol, rosmanol, 12-methoxy-carnosic acid, sageone, and carnosaldehyde using polyamide column, centrifugal partition chromatography, and semi-preparative high performance liquid chromatography. Isolated compounds were screened *in-vitro* for their ability to active the antioxidant response element and general cellular toxicity using mouse primary cortical cultures. All compounds except 12-methoxy-carnosic acid were able to activate the antioxidant response element. Rosmanol was able to dose dependently activate the antioxidant response element without cellular toxicity at the doses tested (12.5, 25, and 50 μM) and thus represents an interesting compound for further studies against neurodegenerative disease.

**Submitted as part of larger publication:** Bioorganic and Medicinal Chemistry

## Introduction

Ethnobotanical investigations of English herbal texts, Indian Ayurvedic medicine, and Chinese traditional medicine report that *S. officinalis* has memory enhancing properties (Perry et al., 1999). *Rosmarinus officinalis* also has a reputation for treatment of nervous system related disorders in European traditional medicine (Heinrich et al., 2006). The essential oil of *Salvia* species including *S. officinalis*, *S. fruticosa*, and *S. lavandulaefolia* displays acetylcholinesterase inhibitory activities (Savelev et al., 2004), which may explain their effects on memory in healthy volunteers (Moss et al., 2010) and mild improvements in cognition shown in a small open labeled trial on patients with Alzheimer's disease (Perry et al., 2003). Extracts of *S. officinalis* have also been shown to improve memory and attention in older (> 65 years of age) healthy volunteers (Scholey et al., 2008).

A number of *Salvia* species and *R. officinalis* are well known to produce the phenolic diterpenes carnosic acid (**1)** and carnosol (**2**) (Abreu et al., 2008). Compounds **1** and **2** are strong antioxidants possessing anti-microbial, anti-cancer, anti-inflammatory, and lipid lowering properties (Bonito et al., 2011; Johnson, 2011). Recently a number of investigations have demonstrated that these compounds also exhibit biological activity which may be useful against neurodegenerative diseases. Protective effects of **2** on dopaminergic neuronal cell lines against rotenone induced toxicity and sodium nitroprusside toxicity in glial cells have been reported (Kim et al., 2006; Kim et al., 2010). Carnosic acid protects against glutamate toxicity in primary rat cortical cultures and against cerebral ischemia in mice by activating the nuclear factor E2-related factor 2 (Nrf2) / Kelch-like ECH-associated protein 1 (Keap1) pathway (Satoh et al., 2008a).

Nrf2 is a transcription factor known to induce a promoter sequence called the antioxidant response element (ARE) which leads to expression of various cytoprotective and antioxidant enzymes such as NQO1. Nrf2 localization and degradation is regulated by its cytoplasmic repressor protein Keap1. In conditions of oxidative stress or disruption by small molecules Nrf2 is freed from Keap1 and enters the nucleus activating the ARE (Itoh et al., 2004). Since many neurodegenerative diseases may be caused or exacerbated by oxidative stress, activation of the ARE is a potential therapeutic strategy (de Vries et al., 2008; Calkins et al., 2009).

Little information is available on the structure activity relationship of phenolic diterpenes for Nrf2/Keap1 activation. Comparisons have been made between **1**, **2**, and a series of alkyl-ester derivatives at carbon 11 and 12 of **1** in HT22 cell lines (Satoh et al., 2008b; Tamaki et al., 2010). Therefore in order to gain further insights into the structure activity of phenolic diterpenes for Nrf2/ARE activation we isolated **1**, **2**, epirosmanol (**3**), rosmanol (**4**), 12-methoxy-carnosic acid (**5**), sageone (**6**), and carnosaldehyde (**7**) from *S. officinalis* (Figure 1). Compounds were screened for Nrf2/ARE activation using transgenic primary mouse cortical cultures modified to express human placental alkaline phosphatase (hPAP) as a reporter gene for ARE. Potential toxicity of the isolated compounds was tested against the cultures using the 3-(4,5-dimethylthiazol-2-

yl)-5-(3-carboxymethoxyphenyl)-2-(4-sulfophenyl) 2H tetrazolium inner salt (MTS) assay.

**Figure 1.** Chemical structures of **1**-**7**

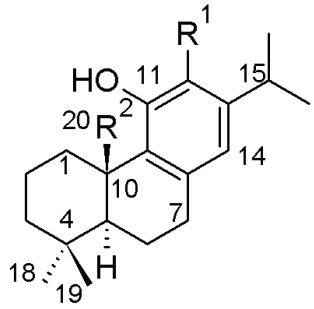


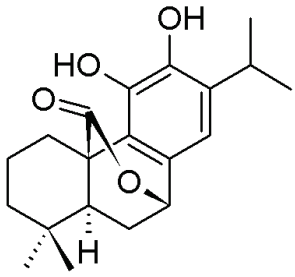


**1** $R^1 = OH, R^2 = COOH$ **2**

**5** $R^1 = OCH_3, R^2 = COOH$

**7** $R^1 = OH, R^2 = CHO$

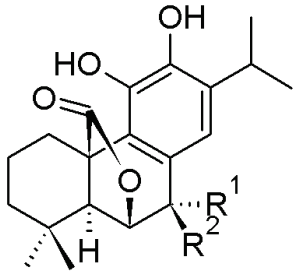


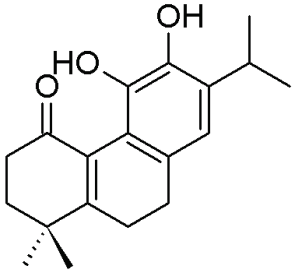


**3** $R^1 = H, R^2 = OH$ **6**

**4** $R^1 = OH, R^2 = H$

**Materials and Methods**

*Plant material*

Dried aerial parts of *Salvia officinalis* were purchased from De Groene Luifel BV, Sluis, Netherlands. A voucher specimen was deposited in the economic botany collection of the National Herbarium Nederland in Leiden under the following barcode: LamiaceaeSalviaofficinalisL.L 0991403J. FischedickNo. 192010.

*Extraction*

Plant material (100 g) was extracted with 2 L acetone for 2 hours to yield 9 g crude extract. The extract was extracted 2 times with 100 mL warm hexane and hexane solution added to polyamide column (100 g). The column was eluted with additional 300 mL of hexane to give 2 g hexane fraction and further eluted with 650 mL MeOH to give 2 g MeOH fraction.

*CPC*

The MeOH and hexane fractions were further purified using a Fast Centrifugal Partition Chromatograph with a 1 L internal volume rotor (Kromaton Technologies, Angers, France). The MeOH fraction was separated by using a two phase solvent system composed of 5 L heptane: acetone: $H_2O$ (3: 5: 2). The MeOH fraction was dissolved in 30 mL 1:1 mixture of upper and lower layers of the solvent system. The CPC system was filled with the lower layer and the phase held in place with a rotor speed of 1000 rpm while the upper layer was pumped into the CPC at a flow rate of 10 mL/min in ascending mode. Equilibrium between the layers was reached when the upper layer began to elute from the CPC (lower layer displaced = 230 mL), after which the sample was immediately injected. After 250 mL of the mobile phase eluted 120 fractions (10 mL each) were collected. The system was then rinsed with 1 L of the remaining lower layer and the eluent collected as an additional rinse fraction. Pressure was stable between 63-65 bar throughout the run. The hexane fraction was separated using a 2 phase solvent system composed of 2.5: 6: 1.5 heptane: acetone: $H_2O$. All other CPC conditions were the same as for the MeOH fraction except the volume of the lower layer displaced during equilibration was 260 mL, the pressure 48 bar, and 80 (10 mL) fractions were collected. Fractions were analyzed by silica gel TLC (hexane: ethyl acetate: acetic acid, 7: 3: 0.1, vanillin/sulfuric acid reagent) and combined based on similarity of profile. Combined fractions from CPC experiment on MeOH fraction are referred to as CPC-M $Fr_{\#}$ and fractions from CPC on hexane fraction as CPC-H $Fr_{\#}$.

*Semi-preparative HPLC*

Final purification was performed on a Shimadzu semi-preparative HPLC. A Luna C18 (2) 100 A 5 micron 250 x 10 mm column was used for separations (Phenomenex, Torrance, CA, USA). $H_2O$ (A) and MeOH (B) were used as mobile phase. Flow rates were 5 mL/min, 10 mL fractions were collected, and UV detector set to 230 and 280 nm. Samples were injected manually using a Rheodyne injector equipped with a 5 mL injection loop.

CPC-M $Fr_{40\text{-}75}$ (660 mg) was dissolved in 10 mL 70% aqueous MeOH and run twice using gradient from 70% B to 85% B in 60 min. Fractions 5, 8-15, and 18-20 were separately combined and MeOH removed under reduced pressure at 40 °C. Combined fractions were then dissolved in 100 mL $H_2O$ and 150 mL EtOAc. The EtOAc layer was collected and solvent removed to yield 12.6 mg **2** from fraction 5, 506.7 mg **1** from fractions 8-15, and 31.4 mg **5** from fractions 18-20. CPC-M rinse

fraction (242 mg) was purified using gradient from 50% B to 100% B in 120 min. Solvent was removed from fractions 7, 9, and 24-25 to yield 2.1 mg **3**, 2.6 mg **4**, and 20.3 mg **2** respectively. CPC-H $Fr_{26-40}$ (164 mg) was dissolved in 5 mL 70% aqueous MeOH and run with gradient from 70% B to 100% B in 120 min. Fractions 9-10 yielded 11.2 mg **6** and fractions 17-18 yielded 5.8 mg **7**. CPC-H $Fr_{41-80}$ (50 mg) was purified under the same conditions as $Fr_{26-40}$ to yield an additional 1.4 mg **6**.

*Structure elucidation*

The structure of isolated compounds was determined by $^1$H-NMR and COSY on a Bruker DMX 500 MHz NMR (Karlsruhe, Germany). An Agilent single quadropole mass spectrometer equipped with an atmospheric pressure chemical ionization probe (APCI) was used for mass confirmation. A 150 x 4.6 mm Luna 5 micron C18 (2) 100A column was used for separation (Phenomenex Inc). Solvent system was composed of MeOH and $H_2O$ plus 0.1% formic acid. The flow rate was 0.5 mL/min. Gradient of 70% MeOH to 100% MeOH in 20 min with 10 min hold at 100% MeOH was used. Mass spectra were acquired in both positive and negative mode with a mass range of 50-500 amu. APCI spray chamber gas temperature was set to 350 °C, a vaporizer temperature of 325 °C, a drying gas flow rate of 5 L/min, and a nebulizer pressure of 40 psig. The VCap was set to 4000 V for positive scans and negative scans while the corona current was 5 µA for positive scans and 15 µA for negative scans.

*Cell cultures*

Primary cortical neuronal cultures were derived from ARE-hPAP reporter mice as previously described (Johnson et al., 2002; Kraft et al., 2004). In brief cortices from E15 mouse pups were pooled in 10 mL ice-cold $Ca^{2+}$ and $Mg^{2+}$ free HBSS (Life Technologies, Carlsbad, CA, USA). Tissue was then minced, centrifuged, and digested in 0.05% trypsin containing no EDTA in HBSS for 15 min at 37 °C. Cells were rinsed 3 times with HBSS following digestion. Then cells were washed with CEMEM (minimum essential media with Earle's salts); (Life Technologies) 2 mM glutamine, 1% penicillin/streptomycin, 10% heat inactivated fetal bovine serum, and 10% horse serum (Atlanta Biologicals, Inc., Lawrenceville, Georgia, USA). Cells were triturated to a single-cell suspension and strained through a 70 µM cell strainer (BD Biosciences, San Jose, California, USA). Cells were counted, assayed for viability using trypan blue, and plated on poly-D-lysine coated plates at a density of 3 x 105 cell/cm$^2$. Cells were kept in CEMEM for 45 min, after which medium was changed with CEMEM. After two days, medium was changed from CEMEM to NBM (Neurobasal media; Life Technologies), supplemented with B27 with antioxidants, and 2 mM glutamine. These mixed cultures (~ 40% astrocytes and 60% neurons) were incubated at 37 °C in a tri-gas incubator with 5% $O_2$, 5% $CO_2$, and 90% $N_2$.

*Bioassay*

After 6 days in culture compounds were dissolved in 100% DMSO (final concentration DMSO 0.1%) and administered to cells for 48 hours. After 48 hours, Nrf2

activation was determined by measuring for hPAP activity as previously described (Kraft et al., 2004). In brief, cells were lysed in TMNC lysis buffer (50 mM Tris, 5 mM MgCl2, 100 mM NaCl, 1% 3-[(3-cholamidopropyl)dimethylammonio]-1-propanesulfonate (CHAPS)) and freeze-thawed at -20 ºC. To inactivate endogenous alkaline phosphatase activity extracts were incubated with 200 mM diethanolamine (DEA) buffer at 65 ºC. The hPAP activity was quantified in 200 mM DEA with 0.8 mM CSPD ((disodium 3-(4-methoxyspiro (1,2-dioxetane-3,2'-(5'-chloro)tricycle(3.3.1.1 $^{3,7}$)decan)-4-yl)phenyl phosphate) (Life technologies), 2x Emerald, and 5 mM $MgCl_2$). Using one second intergration luminescence was measured on a Berthold Orion microplate luminometer (Berthold Technologies GmbH & Co., Bad Wildbad, Germany). Baseline signals from hPAP negative control culture samples (n = 5 for each compound) were subtracted from all values. Cell viability was assayed using the MTS assay following the manufacturer's suggested protocol (Promega, Madison, WI, USA).

*Data analysis*

All data are represented as mean ± SEM (n = 5). Statistical analysis was performed using one-way ANOVA followed by Newman-Keuls multiple comparison (GraphPad Prism, version 4). A P value < 0.05 was considered statistically significant.

**Results and Discussion**

*Isolation*

Phenolic diterpenes **1**-**7** were isolated from an acetone extract of *S. officinalis* by first partitioning hexane soluble material over polyamide, followed by centrifugal partition chromatography, and finally with reverse phased semi-preparative HPLC. Isolated compounds were identified by comparison of $^{1}$H-NMR with literature, confirmed with COSY, and LC-MS (Pukalskas et al., 2005; Cuvelier et al., 1994; Tada et al., 1994). Compound **7** is reported in *S. officinalis* for the first time. All compounds were > 95% pure, except **7** (91%) according to HPLC at 230 nm. Detailed structural data is available in the appendix.

*Bioassay hPAP*

The hPAP expressing primary cortical cultures used in this study have been previously validated as a model system for studying activation of the Nrf2/ARE pathway (Johnson et al., 2002). The positive control *tert*-Butylhydroquinone (tBHQ) has been demonstrated to show Nrf2/ARE dependant neuroprotective effects on such cultures (Kraft et al., 2004). Results of hPAP assays are expressed as the fold increase in hPAP activity over basal levels (Figure 2). The entire hPAP and MTS assay were performed twice with two separate batches of primary cortical cultures in order to understand batch to batch variation in activity. In general the trend in hPAP activity was the same between batches. However in the first batch cells appeared more responsive towards hPAP activation compared with the second batch. This observation could be the result of differences in cell density or ratio of cell types between batches.

**Figure 2.** Fold activation of hPAP levels (compounds **1-7)**. Top first batch, bottom second batch.

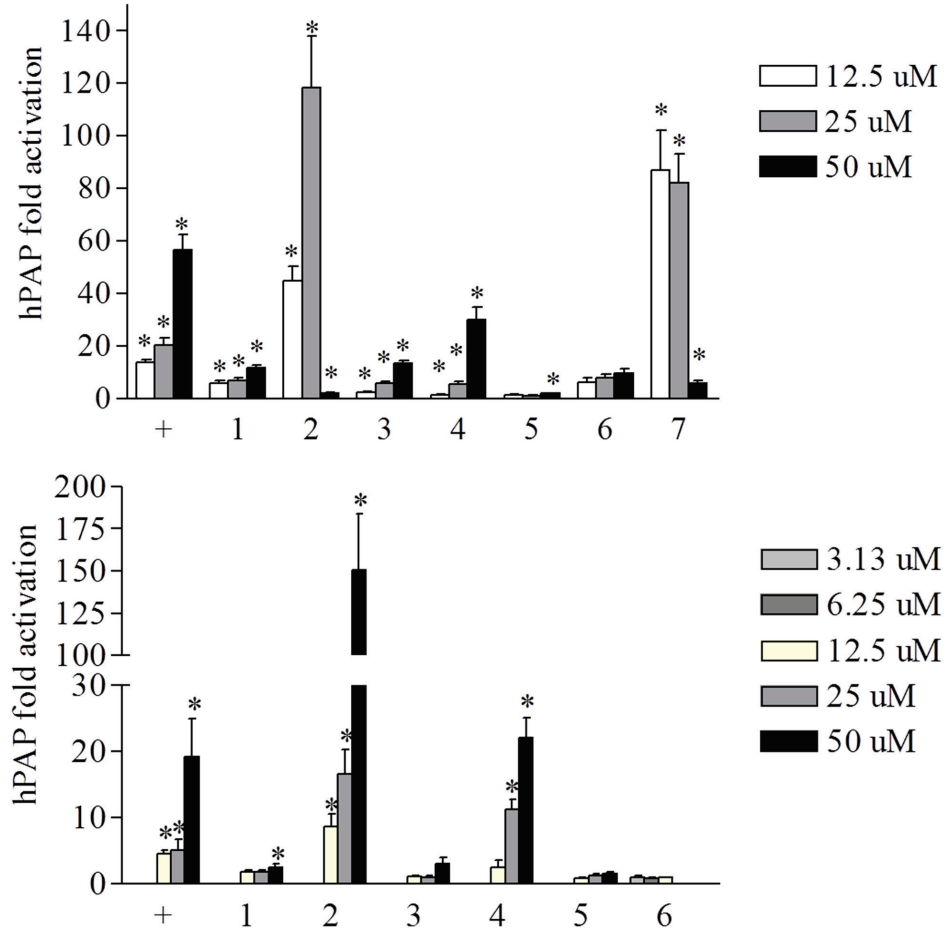


Compounds **2** and **7** were the most potent activators in both hPAP assays (Figure 2). In the first assay, **2** at 25 μM showed > 100 fold increase in hPAP activity and in the second assay at 50 μM > 100 fold increase. Compound **7** had similar levels of hPAP activity at 12.5 and 25 μM. A sharp decrease in hPAP activity was observed at 50 μM for **2** and **7** in the first experiment. Due to poor stability of **7** we were unable to assay this compound in the second batch of cultures. Compound **4** had a similar pattern of hPAP activation as the positive control, tBHQ in both assays. Compounds **1** and **3** had similar and weak patterns of hPAP activation while **5** and **6** were inactive.

**Figure 3.** Cell viability % (compounds **1**-**7**). Top first batch, bottom second batch.

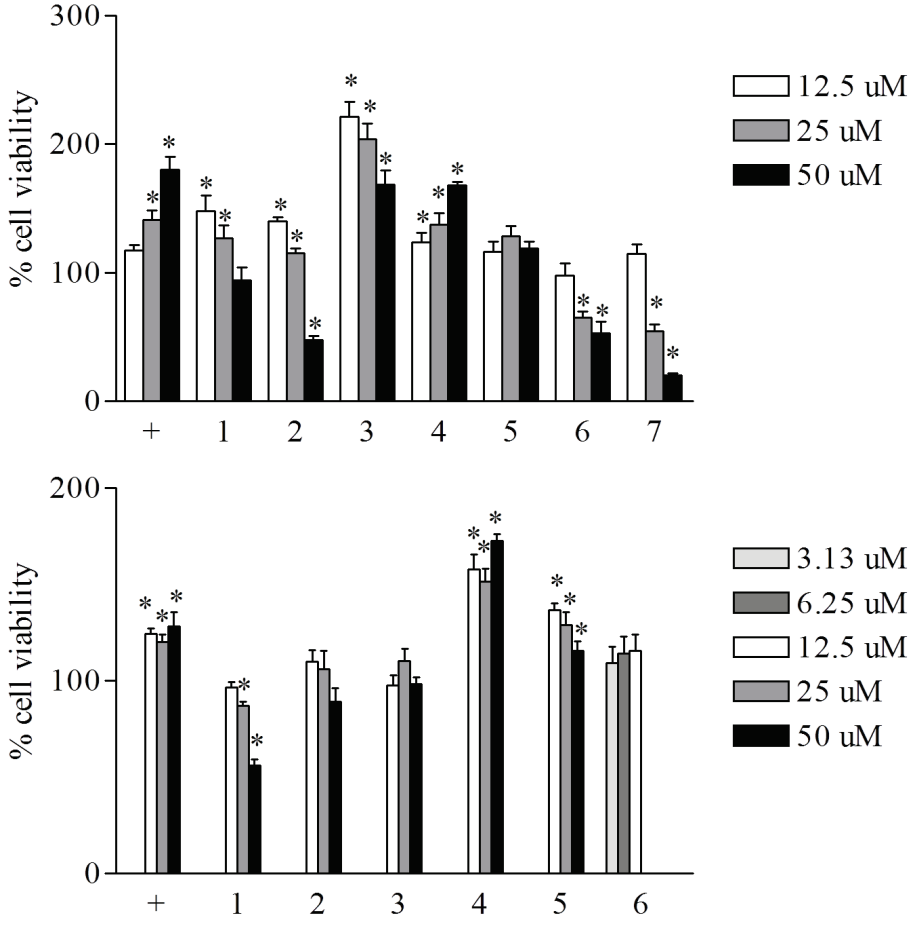


*Bioassay MTS*

Results from the MTS assay are expressed as % cell viability (Figure 3). Significant decrease in cell viability < 100% indicates cellular toxicity while > 100% indicates cell proliferation. Compounds **6** and **7** showed dose dependent decreases in cell viability in the first assay. In the second hPAP and MTS assay **6** was tested at lower doses, 3.13 and 6.25 μM. Although toxicity went away no significant hPAP activity was observed. Compound **2** caused a significant decrease in cell viability to 48% at 50 μM in the first culture batch (Figure 3). The sharp decreases in hPAP activity observed in compounds **2** and **7** at 50 μM in the first batch of cultures are explained by the MTS results demonstrating significant toxicity at such doses. Significant decreases in cell

viability were observed at 25 and 50 μM of **1** in the second batch while a non-significant decrease in viability (94%) at 50 μM was observed in the first batch. Therefore **1** and **2** at lower doses tended to increase or have no effect on cell proliferation while at higher doses decrease cell proliferation or cause toxicity. Compounds **6** and **7** were generally cytotoxic according to MTS results. Both the positive control tBHQ and **4** consistently had significant > 100% cell viability which tended to increase with dosage suggesting the compounds were inducing cell proliferation. Compound **3** was non-toxic in both assays and induced a strong increase in cell viability which decreased at higher doses in the first assay. This effect was not observed in the second assay for **3**. The hPAP inactive compound **5** had a similar pattern of activity as **3** in the MTS assay either dose dependently decreasing cell proliferation or having no effect on cell viability.

*Structure activity relationship*

Previous studies suggested that the mechanism of action of **1** to activate the Nrf2/ARE pathway was due to the catechol moiety initially acting as an antioxidant against reactive oxygen species. Upon oxidation **1** converts into an ortho quinone whose C-14 position can act as an electrophile, reacting with biological thiols such as the cysteine residues of Keap1 thus activating Nrf2 (Satoh et al., 2008a). Another study demonstrated that ester derivatives at both the C-11 and C-12 eliminated activity of **1** (Satoh et al., 2008b). In our experiments a methoxy group at position 12 as in **5** eliminated activity in the hPAP assay, confirming the importance of the catechol moiety for Nrf2/ARE activation. The lack of hPAP activity of **6** could be due to conjugation of the aromatic ring with the 1-carbonyl-5,10-diene functionality which would likely alter the oxidative products formed.

Replacement of the carboxylic acid functionality in **1** with an aldehyde as in **7** caused a dramatic increase in hPAP activity although this was accompanied by dose dependent loss in cell viability. Carnosol and **4** were also much more active than **1** in the hPAP assay. Compound **3**, a stereoisomer of **4**, had weaker activity suggesting that the stereochemistry of the hydroxyl group at position 7 is important. Together these results suggest that an electronegative functionality at the C-7 position can increase Nrf2/ARE activation compared to **1**. However, depending on the functionality it can either increase cell proliferation with higher doses as in **4** or decrease cell viability with higher doses as in **2**. It has been reported that **1** can induce nerve growth factor in human astrocytes and glioblastoma cells regulated by Nrf2 which may explain the potential increases in cell proliferation observed in our experiments (Mimura et al., 2011; Yoshida et al., 2011). A previous comparison of Nrf2/ARE mediated neuroprotection between **1** and **2** in HT22 cells demonstrated more potent activity of **1** compared with **2** (Satoh et al., 2008b). The differences in results are most likely due to differences in the cellular models used. Primary cortical cultures contain a mixture of astrocytes and neurons which are known to display differing patterns of Nrf2/ARE activation (Kraft et al., 2004). Immortalized neuronal cell lines such as HT22 may therefore be of limited use for studying phenolic diterpene mediated Nrf2/ARE activation.

## Conclusions

In conclusion phenolic diterpenes isolated from *S. officinalis* can activate the Nrf/ARE pathway in mouse primary cortical cultures with varied potency. The balance between loss of cell viability and Nrf/ARE activation needs to be carefully considered when studying these compounds as drugs against neurodegenerative diseases. Compounds **1**, **2**, and **7** had a narrow window between doses that activated Nrf/ARE and doses that reduced cell viability. In contrast **4** showed dose dependent increases in Nrf2/ARE activity accompanied by dose dependent increases in cellular proliferation up to 50 μM. These results suggest that **4** is a compound worth further exploration as an agent against neurodegeneration. Finally our results in comparison with literature suggest that different cellular models of Nrf2/ARE activity may lead to different results. Therefore future studies should aim to test a range of active phenolic diterpenes in a variety of models used to study Nrf2/ARE mediated neuroprotection both *in vitro* and *in vivo*.

## Acknowledgements

We would like to thank the European Union Seventh Framework Program for funding the Terpmed project, grant number 227448. This work was also partially funded by R01ES08089 and R01ES10042 from the National Institute of Environmental Health Sciences (JAJ).

**References**

Abreu, M.E., Müller, M., Alegre, L., Munné-Bosch, S., 2008. Phenolic diterpene and α-tocopherol contents in leaf extracts of 60 Salvia species. Journal of the Science of Food and Agriculture 88, 2648–2653.

Bonito, M.C., Cicala, C., Marcotullio, M.C., Maione, F., Mascolo, N., 2011. Biological activity of bicyclic and tricyclic diterpenoids from Salvia species of immediate pharmacological and pharmaceutical interest. Natural Product Communications 6, 1205–1215.

Calkins, M.J., Johnson, D.A., Townsend, J.A., Vargas, M.R., Dowell, J.A., Williamson, T.P., Kraft, A.D., Lee, J.-M., Li, J., Johnson, J.A., 2009. The Nrf2/ARE Pathway as a Potential Therapeutic Target in Neurodegenerative Disease. Antioxidants & Redox Signaling 11, 497–508.

Cuvelier, M.E., Berset, C., Richard, H., 1994. Antioxidant Constituents in Sage (Salvia officinalis). Journal of Agriculture and Food Chemistry 42, 665–669.

de Vries, H.E., Witte, M., Hondius, D., Rozemuller, A.J.M., Drukarch, B., Hoozemans, J., van Horssen, J., 2008. Nrf2-induced antioxidant protection: a promising target to counteract ROS-mediated damage in neurodegenerative disease? Free Radical Biology & Medicine 45, 1375–1383.

Heinrich, M., Kufer, J., Leonti, M., Pardo-de-Santayana, M., 2006. Ethnobotany and ethnopharmacology--interdisciplinary links with the historical sciences. Journal of Ethnopharmacology 107, 157–160.

Itoh, K., Tong, K.I., Yamamoto, M., 2004. Molecular mechanism activating Nrf2-Keap1 pathway in regulation of adaptive response to electrophiles. Free Radical Biology & Medicine 36, 1208–1213.

Johnson, D.A., Andrews, G.K., Xu, W., Johnson, J.A., 2002. Activation of the antioxidant response element in primary cortical neuronal cultures derived from transgenic reporter mice. Journal of Neurochemistry 81, 1233–1241.

Johnson, J.J., 2011. Carnosol: a promising anti-cancer and anti-inflammatory agent. Cancer Letters 305, 1–7.

Kim, S.-J., Kim, J.-S., Cho, H.-S., Lee, H.J., Kim, S.Y., Kim, S., Lee, S.-Y., Chun, H.S., 2006. Carnosol, a component of rosemary (Rosmarinus officinalis L.) protects nigral dopaminergic neuronal cells. Neuroreport 17, 1729–1733.

Kim, S.Y., Park, E., Park, J.A., Choi, B.-S., Kim, S., Jeong, G., Kim, C.-S., Kim, D.K., Kim, S.-J., Chun, H.S., 2010. The plant phenolic diterpene carnosol suppresses sodium nitroprusside-induced toxicity in c6 glial cells. Journal of Agriculture and Food Chemistry 58, 1543–1550.

Kraft, A.D., Johnson, D.A., Johnson, J.A., 2004. Nuclear Factor E2-Related Factor 2-Dependent Antioxidant Response Element Activation by tert-Butylhydroquinone and Sulforaphane Occurring Preferentially in Astrocytes Conditions Neurons against Oxidative Insult. Journal of Neuroscience 24, 1101–1112.

Mimura, J., Kosaka, K., Maruyama, A., Satoh, T., Harada, N., Yoshida, H., Satoh, K., Yamamoto, M., Itoh, K., 2011. Nrf2 regulates NGF mRNA induction by carnosic acid in T98G glioblastoma cells and normal human astrocytes. Journal of Biochemistry 150, 209–217.

Moss, L., Rouse, M., Wesnes, K.A., Moss, M., 2010. Differential effects of the aromas of Salvia species on memory and mood. Human Psychopharmacology 25, 388–396.

Perry, N.S.L., Bollen, C., Perry, E.K., Ballard, C., 2003. Salvia for dementia therapy: review of pharmacological activity and pilot tolerability clinical trial. Pharmacology, Biochemistry, and Behavior 75, 651–659.

Perry, E.K., Pickering, A.T., Wang, W.W., Houghton, P.J., Perry, N.S., 1999. Medicinal plants and Alzheimer's disease: from ethnobotany to phytotherapy. Journal of Pharmacy and Pharmacology 51, 527–534.

Pukalskas, A., van Beek, T.A., de Waard, P., 2005. Development of a triple hyphenated HPLC-radical scavenging detection-DAD-SPE-NMR system for the rapid identification of antioxidants in complex plant extracts. Journal of Chromatography A 1074, 81–88.

Savelev, S.U., Okello, E.J., Perry, E.K., 2004. Butyryl- and acetyl-cholinesterase inhibitory activities in essential oils of Salvia species and their constituents. Phytotherapy Research 18, 315–324.

Scholey, A.B., Tildesley, N.T.J., Ballard, C.G., Wesnes, K.A., Tasker, A., Perry, E.K., Kennedy, D.O., 2008. An extract of Salvia (sage) with anticholinesterase properties improves memory and attention in healthy older volunteers. Psychopharmacology 198, 127–139.

Satoh, T., Kosaka, K., Itoh, K., Kobayashi, A., Yamamoto, M., Shimojo, Y., Kitajima, C., Cui, J., Kamins, J., Okamoto, S., Izumi, M., Shirasawa, T., Lipton, S.A., 2008a. Carnosic acid, a catechol-type electrophilic compound, protects neurons both in vitro and in vivo through activation of the Keap1/Nrf2 pathway via S-alkylation of targeted cysteines on Keap1. Journal of Neurochemistry 104, 1116–1131.

Satoh, T., Izumi, M., Inukai, Y., Tsutsumi, Y., Nakayama, N., Kosaka, K., Shimojo, Y., Kitajima, C., Itoh, K., Yokoi, T., Shirasawa, T., 2008b. Carnosic acid protects neuronal HT22 Cells through activation of the antioxidant-responsive element in free carboxylic acid- and catechol hydroxyl moieties-dependent manners. Neuroscience Letters 434, 260–265.

Tada, M., Okuno, K., Chiba, K., Ohnishi, E., Yoshii, T., 1994. Antiviral diterpenes from Salvia officinalis. Phytochemistry 35, 539–541.

Tamaki, Y., Tabuchi, T., Takahashi, T., Kosaka, K., Satoh, T., 2010. Activated glutathione metabolism participates in protective effects of carnosic acid against oxidative stress in neuronal HT22 cells. Planta Medica 76, 683–688.

Yoshida, H., Mimura, J., Imaizumi, T., Matsumiya, T., Ishikawa, A., Metoki, N., Tanji, K., Ota, K., Hayakari, R., Kosaka, K., Itoh, K., Satoh, K., 2011. Edaravone and carnosic acid synergistically enhance the expression of nerve growth factor in human astrocytes under hypoxia/reoxygenation. Neuroscience Research 69, 291–298.

# Appendix Chapter 7

**Table A1.** $^{1}$H-NMR data [$\delta_H$ (J, Hz)] $CDCl_3$ 500 MHz (compounds **1**, **5**, **7**)

| **$^{1}$H** | **carnosic acid** | **12-methoxy-carnosic acid** | **carnosaldehyde** |
|---|---|---|---|
| 1α | 1.25-1.3 m | 1.23 m | 1.13 m |
| 1β | 3.31 dt (3.6, 13.8) | 3.56 m | 3.22 m |
| 2α | 1.76 dddd (3.5, 8.7, 13.5, 17.1) | 2.19 qt (4.5, 14.6) | 1.48-1.59* m |
| 2β | 1.49 br d (13.3) | 1.59 m | 1.48-1.59* m |
| 3α | 1.57-1.65 m | 1.54 m | 1.15-1.36* m |
| 3β | 1.3-1.36 m | 1.30 m | 1.15-1.36* m |
| 5 | 1.59 dd (1.7, 12.7) | 1.56 m | 1.62 dd (1.7, 12.7) |
| 6α | 1.88 m | 1.85 m | 2.03 m |
| 6β | 2.34 tdd (7.0, 10.8, 12.9) | 2.28 tdd (6.5, 11.1, 12.9) | 1.86 tt (8.7, 13.2) |
| 7α | 2.83 m | 2.84 m | 2.87 dd (3.6, 8.5) |
| 7β | 2.83 m | 2.84 m | 2.87 dd (3.6, 8.5) |
| 14 | 6.57 s | 6.53 s | 6.60 s |
| 15 | 3.19 hept (6.9) | 3.17 hept (6.9) | 3.23 m |
| 16 | 1.21 d (6.9) | 1.21 d (6.9) | 1.21 d (6.9) |
| 17 | 1.22 d (6.9) | 1.21 d (6.9) | 1.21 d (6.9) |
| 18 | 1.01 s | 0.98 s | 1.04 s |
| 19 | 0.92 s | 0.89 s | 0.9 s |
| 20 | | | 9.9 d (1.5) |
| OH | ~7.09 br s | | 7.13 s |
| OH | ~5.71 br s | ~6.11 br s | 5.78 s |
| O-Me | | 3.73 s | |

*Signals difficult to assign due to peak overlap. Calibrated to 7.26 ppm.

**Table A2.** $^{1}$H-NMR data [$\delta_H$ (J, Hz)] $CDCl_3$ 500 MHz (compound **6**). Calibrated to 7.26 ppm.

| $^{1}$H | sageone |
|---|---|
| 2 | 2.69 t (7) |
| 3 | 1.94 t (7) |
| 6 | 2.39 dd (5.9, 8.1) |
| 7 | 2.54 dd (5.9, 8) |
| 14 | 6.58 s |
| 15 | 3.29 hept (6.9) |
| 16 | 1.24 d (6.9) |
| 17 | 1.24 d (6.9) |
| 18 | 1.27 s |
| 19 | 1.27 s |
| OH | 9.44 s |
| OH | 6.16 s |

**Table A3.** LC-MS data, APCI ion (percent abundance)

| compound | APCI positive [M+H] | APCI negative [M-H] |
|---|---|---|
| carnosic acid | not detected | 331 (100) |
| carnosol | 331 (80) | 329 (100) |
| epirosmanol | 347 (10) | 345 (100) |
| rosmanol | 347 (10) | 345 (100) |
| 12-methoxy-carnosic acid | not detected | 345 (100) |
| sageone | 301 (100) | 299 (100) |
| carnosaldehyde | 317 (55) | 315 (100) |

**Table A4.** $^{1}$H-NMR data [$\delta_H$ (J, Hz)] MeOD 500 MHz (compounds **2**-**4**)

| **$^{1}$H** | **carnosol** | **epirosmanol** | **rosmanol** |
|---|---|---|---|
| 1α | 2.81 br dd (1.4, 14.3) | 2.78 br d (14.3) | 1.97 td (5.3, 14.1) |
| 1β | 2.57 td (4.4, 14) | 2.57 td (4.4, 14) | 3.30 * |
| 2α | 1.9 m | 1.85 dtd (3.1, 10.8, 13.8) | 1.62 m |
| 2β | 1.6 ddt (3.3, 7.2, 13.8) | 1.6 m | 1.52 m |
| 3α | 1.52 br dd (1.2, 13.1) | 1.49 br d (13.2) | 1.26 m |
| 3β | 1.32 td (3.3, 13.6) | 1.32 dt (6.9, 13.6) | 1.45 m |
| 5 | 1.7 dd (5.7, 10.7) | 1.38 d (4.1) | 2.26 s |
| 6α | 1.85 m | 4.3 dd (4.2, 4.3) | 4.52 d (3.3) |
| 6β | 2.19 m | | |
| 7α | 5.42 br d (2.9) | 5.13 d (4.5) | |
| 7β | | | 4.59 d (3.3) |
| 14 | 6.69 s | 6.77 s | 6.84 s |
| 15 | 3.24 hept* | 3.26 hept* | 3.22 hept (7.1) |
| 16 | 1.20 d (6.2) | 1.22 d (6.1) | 1.22 d (6.9) |
| 17 | 1.19 d (6.5) | 1.21 d (6.5) | 1.19 d(6.9) |
| 18 | 0.88 s | 1.03 s | 1.03 s |
| 19 | 0.87 s | 0.91 s | 0.91 s |
| OH | ~7.87 br | | |
| OH | ~4.57 br | | |

*Signals obscured by solvent. Calibrated to 3.31ppm

**Figure A1.** $^{1}$H-NMR spectra of carnosic acid (**1**) 500 MHz $CDCl_3$

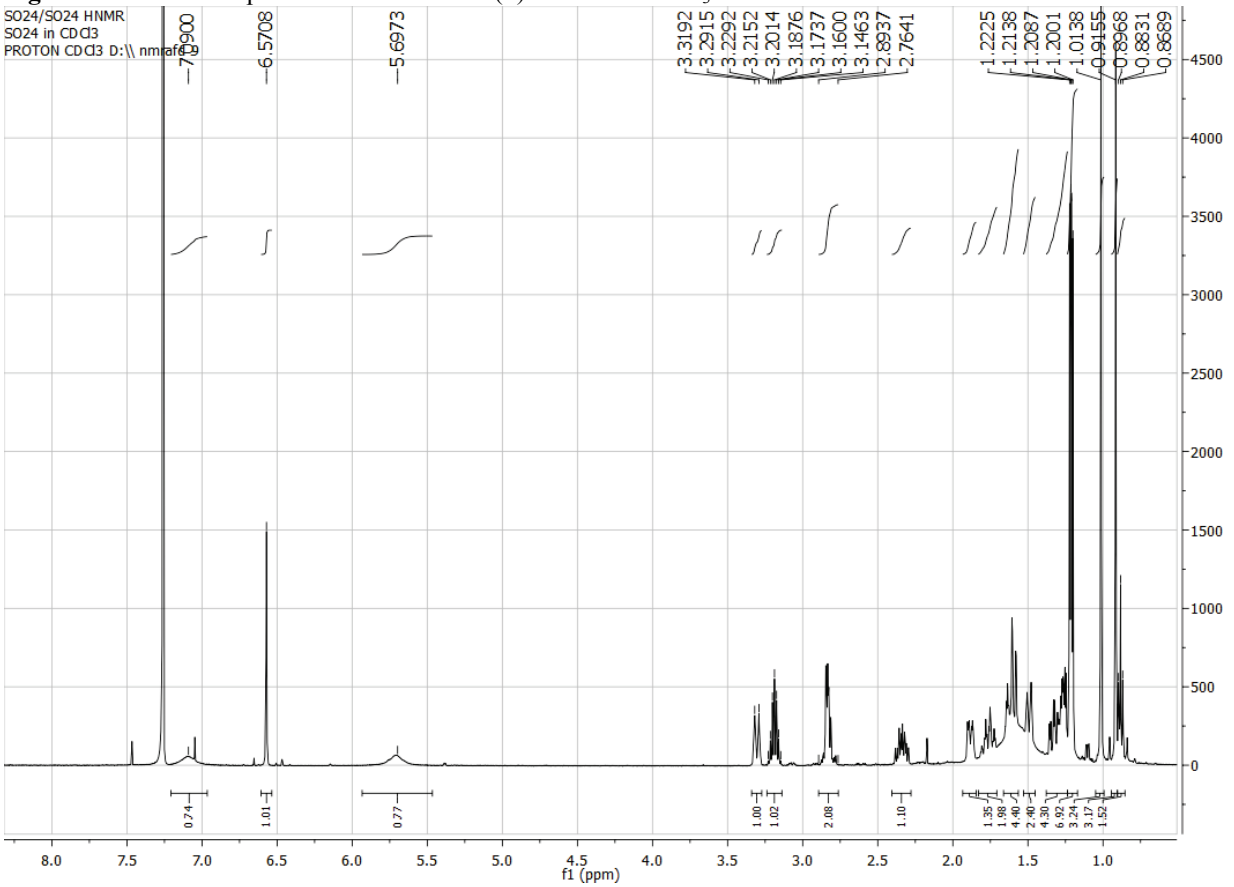

**Figure A2.** [1]H-NMR spectra of carnosol (**2**) 500 MHz MeOD

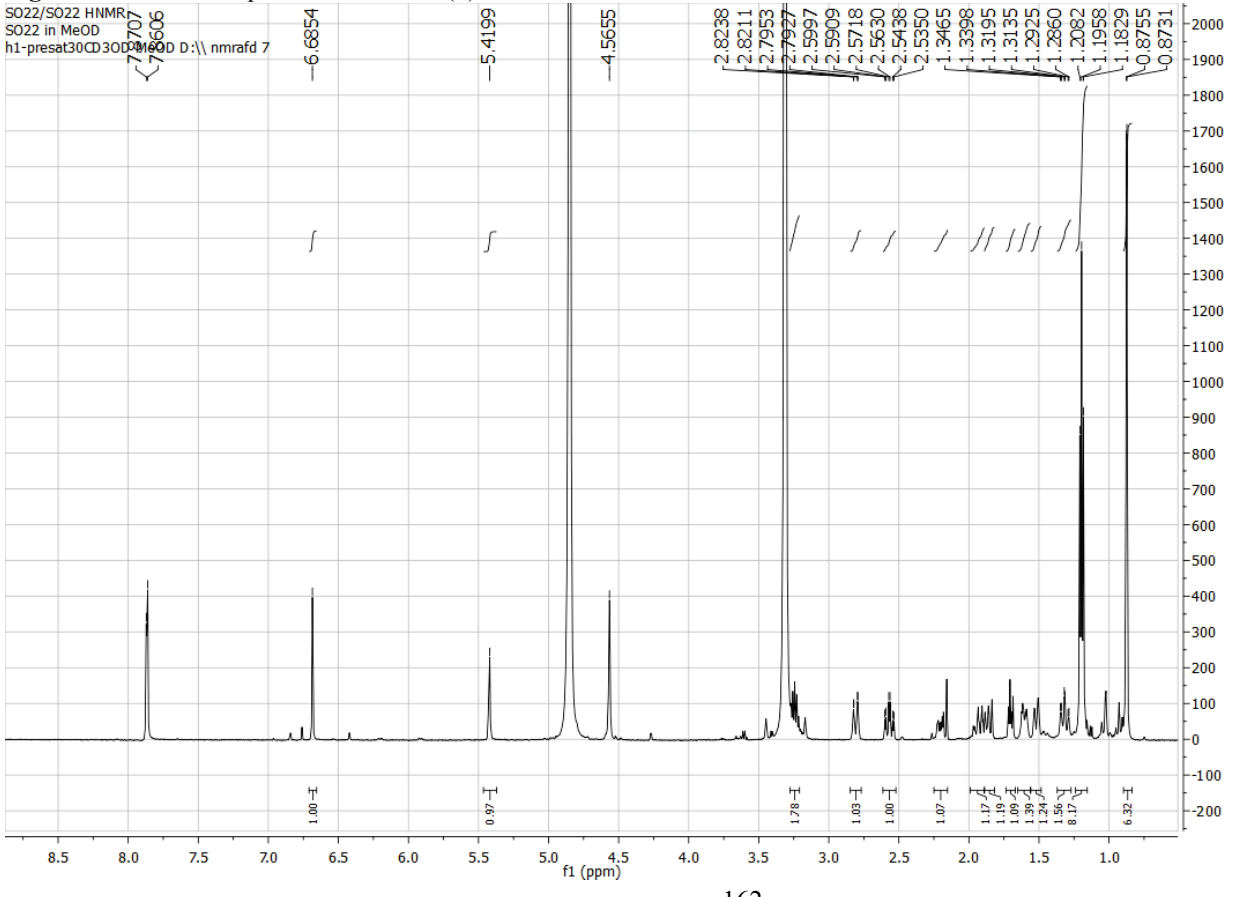

**Figure A3.** [1]H-NMR spectra of epirosmanol (**3**) 500 MHz MeOD

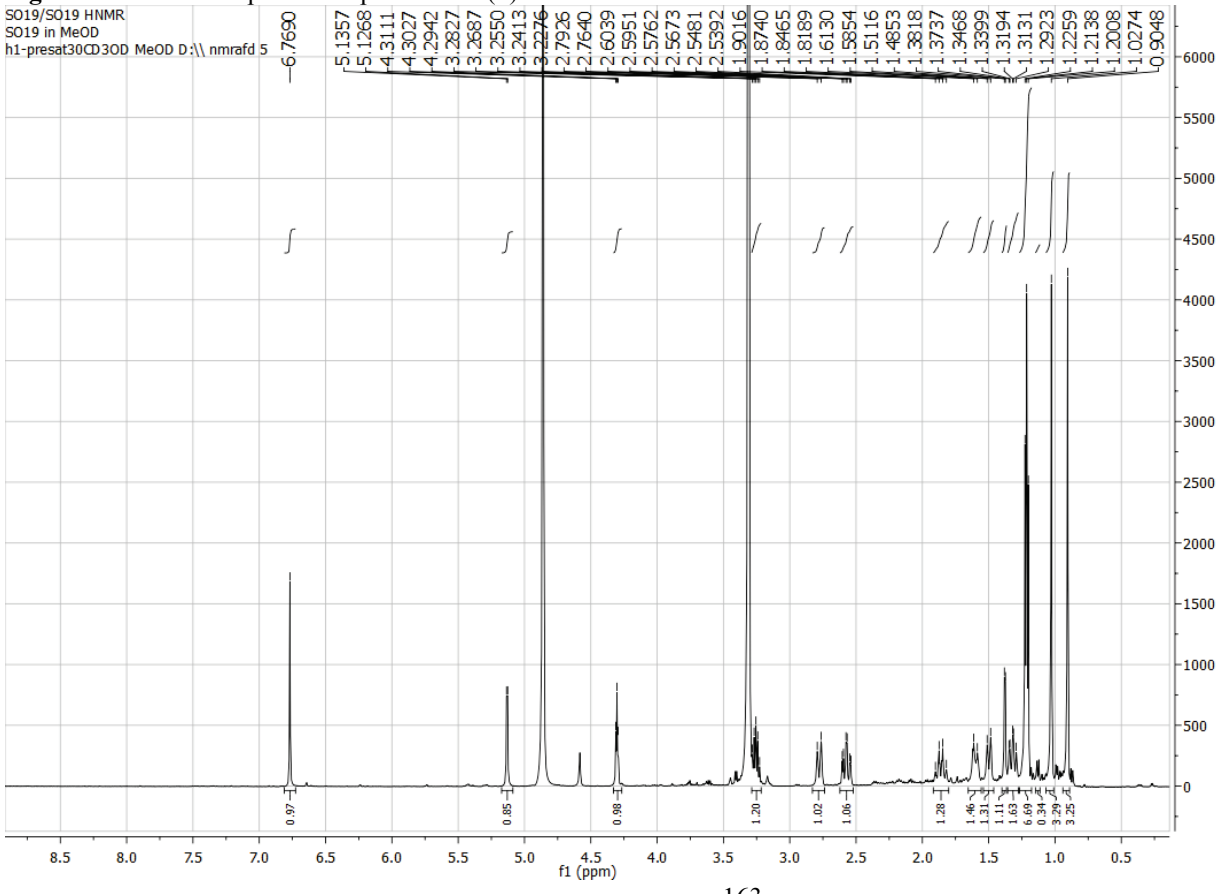

**Figure A4.** [1]H-NMR spectra of rosmanol (**4**) 500 MHz MeOD

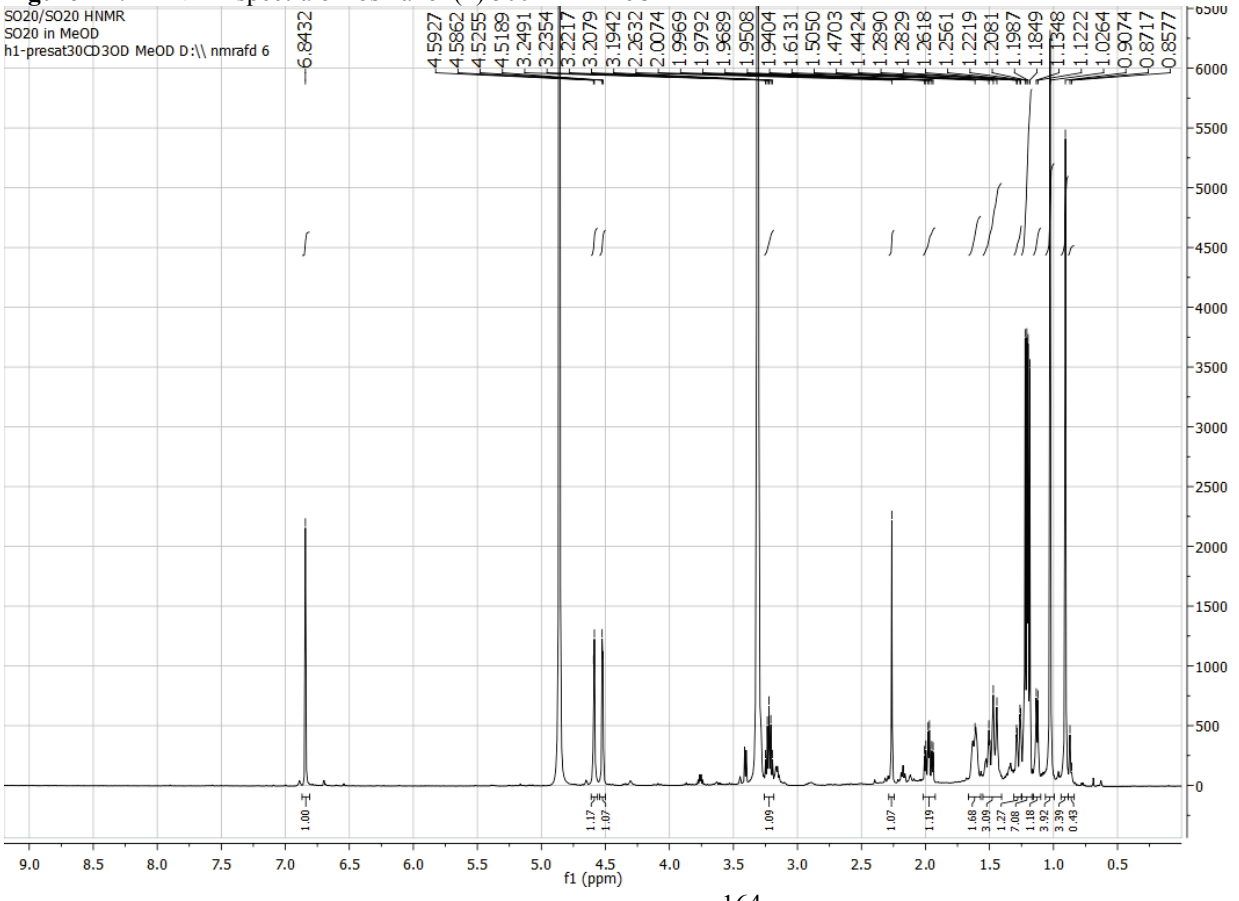

**Figure A5.** $^{1}$H-NMR spectra of 12-methoxy-carnosic acid (**5**) 500 MHz $CDCl_3$

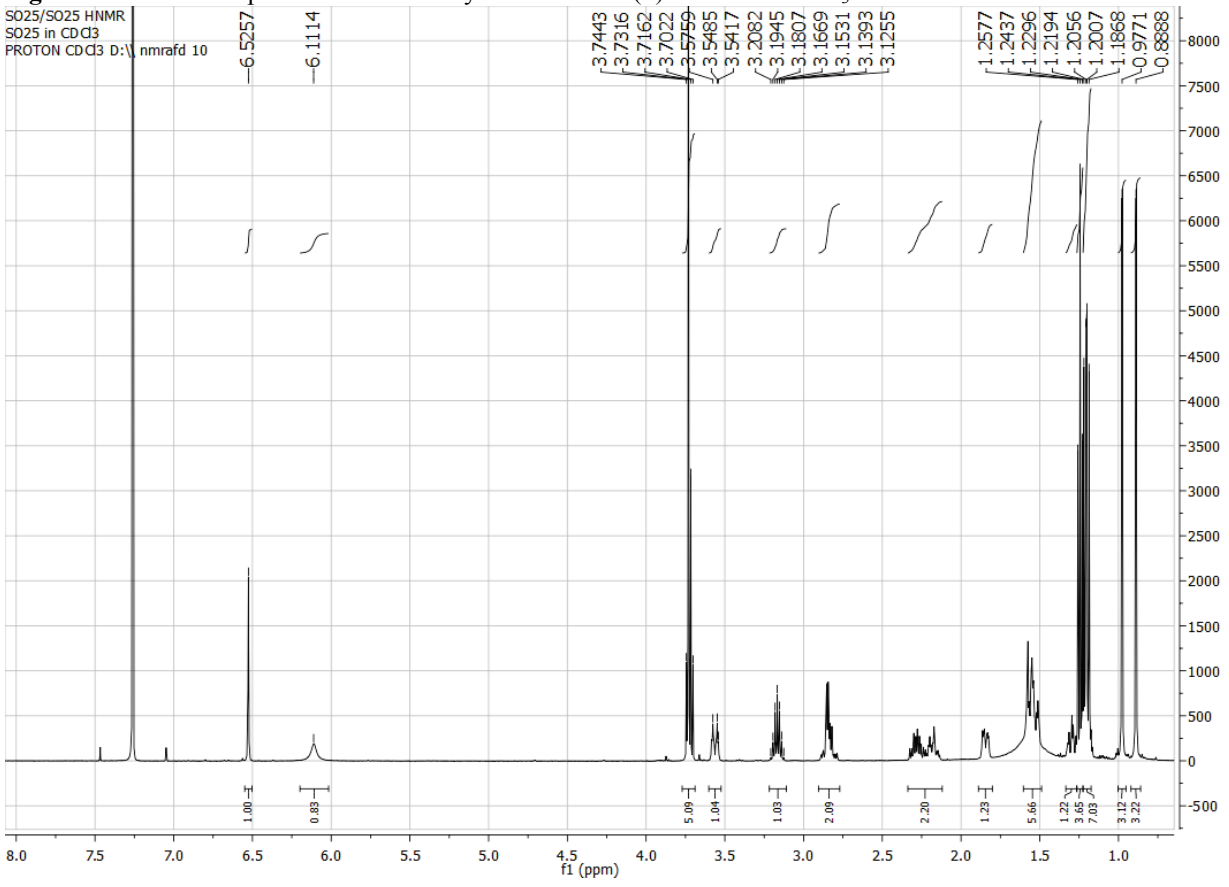

**Figure A6.** $^{1}$H-NMR spectra of sageone (**6**) 500 MHz $CDCl_3$

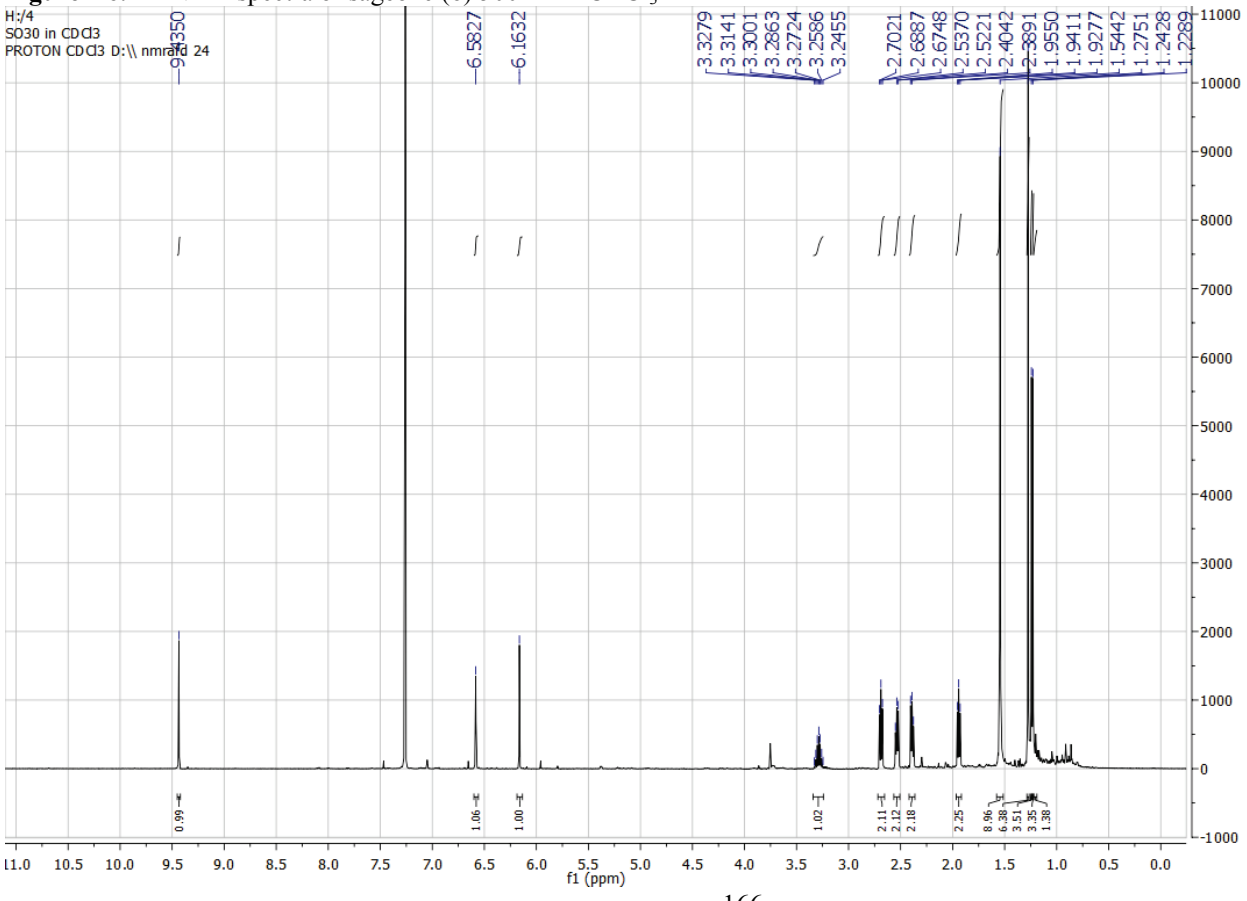

**Figure A7.** $^{1}$H-NMR spectra of carnosaldehyde (**7**) 500 MHz $CDCl_3$